MID-AMERICA TRANSPORTATION CENTER

Report # MATC-MS&T: 132-3

Final Report

WBS: 25-1121-0005-132-3

SMART Shear Keys for Multi-Hazards Mitigation of Diaphragm-Free Girder Bridges - Phase III

Haibin Zhang, PhD
Associate Professor, School of Civil Engineering and Architecture, Hainan University
Research Consultant, Department of Civil, Architectural, and Environmental Engineering, Missouri University of Science and Technology

Junyi Huang
Research Assistant
School of Civil Engineering and Architecture
Hainan University

Genda Chen, PhD, PE, F.ASCE
Professor and Robert W. Abbett Distinguished Chair in Civil Engineering
Department of Civil, Architectural, and Environmental Engineering
Missouri University of Science and Technology

2024

A Cooperative Research Project sponsored by U.S. Department of Transportation- Office of the Assistant Secretary for Research and Technology

SMART Shear Keys for Multi-Hazards Mitigation of Diaphragm-Free Girder Bridges – Phase III

Haibin Zhang, Ph.D.
Research Consultant
Department of Civil, Architectural, and Environmental Engineering
Missouri University of Science and Technology

Junyi Huang,
Research Assistant
School of Civil Engineering and Architecture
Hainan University

Genda Chen, Ph.D.
Robert W. Abbett Distinguished Professor in Civil Engineering
Department of Civil, Architectural, and Environmental Engineering
Missouri University of Science and Technology

A Report on Research Sponsored by

Mid-America Transportation Center

University of Nebraska–Lincoln

September 2024

Technical Report Documentation Page

1. Report No. 25-1121-0005-132-3	2. Government Accession No.	3. Recipient's Catalog No.
4. Title and Subtitle SMART Shear Keys for Multi-Hazards Mitigation of Diaphragm-Free Girder Bridges – Phase III		5. Report Date September 2024
		6. Performing Organization Code
7. Author(s) Haibin Zhang, Junyi Huang, Genda Chen		8. Performing Organization Report No. 25-1121-0005-132-
9. Performing Organization Name and Address Center for Intelligent Infrastructure Department of Civil, Architectural, and Environmental Engineering Missouri University of Science and Technology 500 W. 16th St. Rolla, MO 65409-0810		10. Work Unit No. (TRAIS)
		11. Contract or Grant No. 69A3551747107
12. Sponsoring Agency Name and Address Office of the Assistant Secretary for Research and Technology 1200 New Jersey Ave., SE Washington, D.C. 20590		13. Type of Report and Period Covered January 2020 – March 31, 2024
		14. Sponsoring Agency Code MATC TRB RiP No. 91994-52
15. Supplementary Notes		

16. Abstract

To mitigate multiple natural hazards such as earthquakes and tsunamis, sliding, modular, adaptive, replaceable, and two-dimensional (SMART) shear keys were proposed as fuse elements between bridge superstructures and substructures. These elements aim to adaptively control both forces and displacements under different loads. This Phase III study focuses on the computational model and tsunami response of a 1/5-scale bridge including four SMART shear keys in a large flume. ANSYS software was used to establish a three-dimensional finite element model of the bridge and shear keys. To simulate tsunamis, solitary waves were applied as boundary conditions in the computational model with a wave height of 0.57 to 0.87 m. This range covers the typical wave heights expected during tsunami events. For 0.72 m wave height, a friction coefficient of 0.275 to 0.375 at the interface of four shear key modules were considered to investigate their impact on the bridge behavior. The dynamic response of the bridge model increases with the height of tsunami waves. At 0.72 m, the friction coefficient has a notable effect on the dynamic response of the bridge. The higher the friction coefficient, the greater the energy dissipation, thus reducing the maximum stress and displacement in the shear keys. The design of SMART shear keys can be optimized for different wave heights and friction coefficients to improve the overall safety and performance of bridges under tsunami loads. This study demonstrates the effective use of computational mechanics in evaluating the performance of shear keys under varying wave heights and friction coefficients.

17. ORCID No. of each Researcher Haibin Zhang: 0000-0003-4318-8202 Genda Chen: 0000-0002-0658-4356	18. Distribution Statement		
19. Security Classif. (of this report) Unclassified	20. Security Classif. (of this page) Unclassified	21. No. of Pages 40	22. Price

Table of Contents

List of Figures

List of Tables

Acknowledgments

We appreciate the strong support provided by laboratory technicians in the Department of Civil, Architectural, and Environmental Engineering at Missouri University of Science and Technology. The authors would also like to thank Ms. Rebekah Miller and Dr. Tim Maddux for their assistance during test setup and data acquisition. Thanks are due to graduate students and postdocs supervised by Dr. Genda Chen for their support during laboratory tests.

Disclaimer

The contents of this report reflect the views of the authors, who are responsible for the facts and the accuracy of the information presented herein. This document is disseminated in the interest of information exchange. The report is funded, partially or entirely, by a grant from the U.S. Department of Transportation's University Transportation Centers Program. However, the U.S. Government assumes no liability for the contents or use thereof.

Executive Summary

To mitigate multiple natural hazards such as earthquakes and tsunamis, sliding, modular, adaptive, replaceable, and two-dimensional (SMART) shear keys were proposed as fuse elements between bridge superstructures and substructures. These elements aim to adaptively control both forces and displacements under different loads. This Phase III study focuses on the computational model and tsunami response of a 1/5-scale bridge including four SMART shear keys in a large flume. ANSYS software was used to establish a three-dimensional finite element model of the bridge and shear keys. To simulate tsunamis, solitary waves were applied as boundary conditions in the computational model with a wave height of 0.57 to 0.87 m. This range covers the typical wave heights expected during tsunami events. For a 0.72 m wave height, a friction coefficient of 0.275 to 0.375 at the interface of four shear key modules were considered to investigate their impact on the bridge behavior. The dynamic response of the bridge model increases with the height of tsunami waves. At 0.72 m, the friction coefficient has a notable effect on the dynamic response of the bridge. The higher the friction coefficient, the greater the energy dissipation, thus reducing the maximum stress and displacement in the shear keys. The design of SMART shear keys can be optimized for different wave heights and friction coefficients to improve the overall safety and performance of bridges under tsunami loads. This study demonstrates the effective use of computational mechanics in evaluating the performance of shear keys under varying wave heights and friction coefficients.

Chapter 1 Introduction

1.1 Objective

The most destructive hazard in coastal areas are tsunamis caused by large-scale water movements resulting from earthquakes, submarine landslides, and landslides. Such hazards can cause substantial economic losses and many casualties in coastal areas. Coastal bridges are critical links of a road transportation network and often subjected to tsunamis. Tsunamis induce significant hydrodynamic loads on the deck of encountered bridges in the form of waves. When the hydrodynamic loads exceed the capacity of bridge superstructures, the bridge superstructures will be displaced from its substructure supports. According to the New York State Department of Transportation, about 58% of the U.S. bridges that collapsed during 1966 - 2005 were caused by hydraulic hazards, such as the hydrodynamic effects resulting from tsunamis. Between 1900 and 2020, over 700 tsunamis triggered by earthquakes occurred worldwide, resulting in an average wave height of 2.3 m (Reid and Mooney, 2023). Tsunami waves following the 2004 Indian Ocean, 2010 Chile, and 2011 Japan earthquakes resulted in transverse offset and overturning of bridge decks (Reid and Mooney, 2023).

Conventional shear keys used in bridges provide lateral support to the bridge superstructure to prevent damage from falling beams. Recently, the concept of SMART shear keys has been proposed as sacrificial elements to reduce potential damage of cap girders and piers caused by extreme hydrodynamic actions through sliding shear failures. The working principle of SMART shear keys and their performance under tsunami actions were recently

investigated through physical experiments. However, more detailed investigations are needed as the following gaps still exist. That is, the effects of dowel bar strength and the inclination angle of the contact surface between individual modules on the performance of the shear key is unknown, particularly, under tsunami loading.

The main objectives of this research project are to develop a computational model of the 1/5-scale coastal highway bridge, simulate its dynamic responses under tsunami loads, and understand its underlying behavior in dowel bars and the friction surface of SMART shear keys. The results of this project will extend the understanding of the bridge model from recent and limited physical experiments.

1.2 Literature Review on Shear Keys

1.2.1 Design concept and category

Shear keys play a vital role in bridge structures by regulating the lateral displacement of bridge decks when subjected to earthquake and other external forces. Shear keys are generally located between the superstructure (e.g., girders beneath decks) and the substructure (e.g., piers or abutments) of a bridge and serve to effectively connect the two parts and transfer loads. According to the current California Bridge Design Code (CALTRANS, 2019), the transfer of lateral seismic forces to the abutment piles is controlled by the design of the shear key such that the maximum shear capacity of the shear key does not exceed the lesser of 30% of the dead load vertical reaction at the abutment and 75% of the total shear capacity of the pile plus the shear capacity of one of the wing-walls. In this design

approach, the sacrificial shear keys are anticipated to undergo failure initially, causing minimal and repairable damage to the abutment walls.

Shear keys can be classified into two types based on their location: external and internal shear keys, as shown in Figure 1.1 and Figure 1.2 . They can also be divided into monolithic and isolated shear keys, as shown in Figure 1.3 and Figure 1.4, respectively, depending on the interface difference between them and supporting abutments/cap beams.

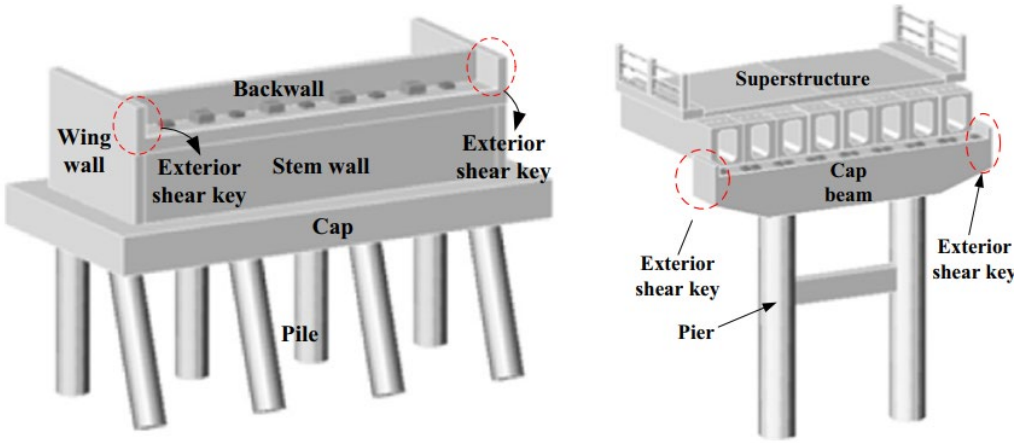

(a) Abutment (b) Cap beam

Figure 1.1 Exterior shear keys at (a) abutment and (b) cap beam (Han et al., 2017)

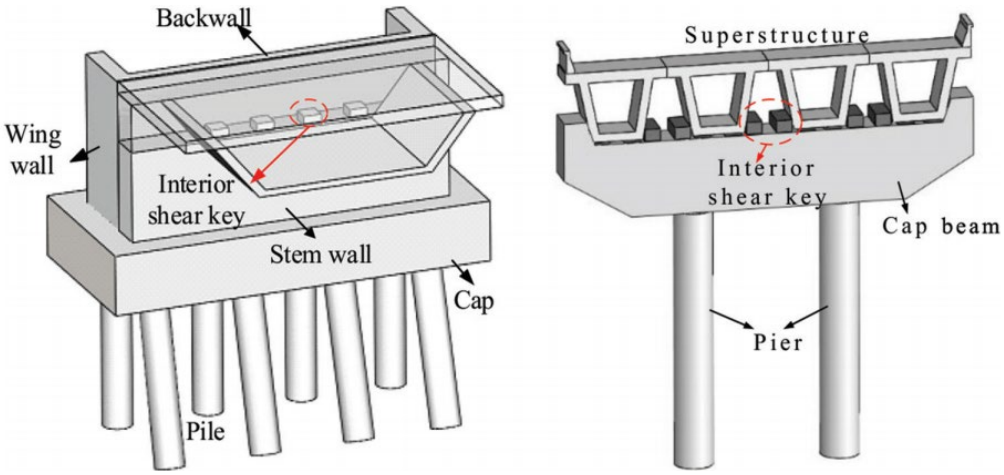

(a) Abutment (b) Cap beam

Figure 1.2 Interior shear keys at (a) abutment and (b) cap beam (Han et al., 2018)

(a) Monolithic shear key (b) Isolated shear key

Figure 1.3 Exterior shear keys: (a) monolithic and (b) isolated (Kottari et al., 2020)

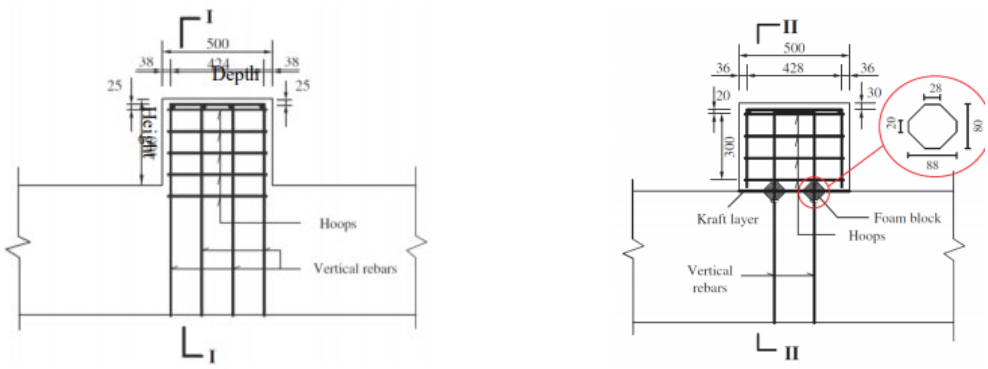

(a) Monolithic shear key (b) Isolated shear key

Figure 1.4 Interior shear keys: (a) monolithic and (b) isolated (Han et al., 2018)

1.2.1.1 Exterior sacrificial shear keys

Megally et al. (2001) presented an experimental program that investigated the performance of external sacrificial shear keys for six bridge abutments under simulated seismic loading. Variables in the external shear key tests included the back and wing walls, the use of different key details, and the post-tensioning of the abutment pole walls. Based on the test results, it was shown that the piles and wing walls of the abutments were at high risk of significant damage. Significant damage to the abutment walls or the piles beneath them is undesirable as it makes post-earthquake repair difficult and may require reconstruction of the abutment walls. Therefore, the use of shear keys as a means of controlling damage to the piles is practically non-conservative for the design of sacrificial shear keys. A two-spring component hysteresis analysis model was developed based on experimental results, and mathematical rules describing the hysteresis model were given. The analysis shows that the shear friction model used in CALTRANS Design Specifications is non-conservative for the design of sacrificial shear keys, which may lead to overloading of bearing and support piles.

Bozorgzadeh et al. (2006) conducted an experimental research program at the University of California, San Diego to better understand the seismic performance of sacrificial external shear keys for bridge abutments according to CALTRANS Specifications by designing and constructing ten external shear keys at a scale of 1:2.5 with different types of connections between shear keys and abutments and varying reinforcement interfaces. The primary objective of the research program was to reassess the validity of the design equations to estimate the capacity of the shear keys within a capacity design framework. A secondary

objective was to provide data to develop analytical models that could be used to accurately estimate shear key capacity, and finally, to provide appropriate reinforcement details and preparation of construction joint faces at the shear key-rod wall interface to allow the shear keys to function as a structural fuse. The experimental results indicate that smooth construction joints should be used to allow sliding shear damage to occur at the shear key-abutment rod wall interface. In addition, a mechanistic model for the evaluation of the sliding shear damage capacity was developed for assessing the ability of exterior shear keys against the slide shear damage.

An experimental evaluation was carried out by Silva et al. (2009) to study the as-built sacrificial external shear keys for various construction joint types and to analyze their load-displacement response at peak and post-peak phases under cyclic loading. Based on the experimental results, a hysteretic model with a two-spring component with gap and strength degradation was developed. This model accurately replicated the cyclic response of shear keys, including their stiffness and capacity degradation, which were caused by the loss of aggregate interlocking and the fracture of the reinforcement.

Han et al. (2017) presented an experimental study on the seismic performance of reinforced concrete (RC) sacrificial exterior shear keys, considering the effects of reinforcement ratio and the type of construction joint. Three failure modes of the shear key under reversed loads were outlined, with the introduction of two analytical models for forecasting the force-displacement backbone curve. These models demonstrated a strong correlation with experimental findings.

Kottari et al. (2020) introduced a novel design approach aimed at mitigating the abrupt and unpredictable diagonal shear failure often observed in conventional monolithic exterior shear keys. This method facilitates a more controlled failure mechanism, where the horizontal sliding of the shear key takes precedence over the diagonal cracking of the stem wall. The experimental results have confirmed the validity of the analytical formulas and design methodology.

1.2.1.2 Interior sacrificial shear keys

Megally et al. (2001) examined how seven interior shear keys responded to seismic activity. The experiment explored various loading protocols, geometric aspect ratios, and reinforcement ratios of the shear keys. The findings indicated that the performance of interior shear keys is minimally impacted by factors such as load history, aspect ratio, and reinforcement ratio. However, the aspect ratio influenced the deterioration of cyclic friction loading and observed levels of damage. Greater aspect ratios resulted in reduced degradation of the friction load.

Han et al. (2018, 2020) primarily explored the seismic behaviors, damage modes, and load transfer mechanisms of internal shear keys subjected to cyclic transverse loading reversals. They then implemented suitable construction fuses at the interface between the shear key and the cap beam to guarantee their effectiveness as structural fuses. Furthermore, a computational model was formulated for analyzing the load-displacement behavior of shear keys in various types of structural fuses, aiming to accurately forecast their response. The seismic capacity of six interior shear key specimens was assessed with varying main

parameters such as the number and ratio of vertical bars, hoop ratio, shear span ratio, loading height, and presence of construction joints. Three distinct failure modes were observed in the interior shear key specimens during the experiments. Additionally, distinct analytical frameworks were devised for the three failure modes, along with an empirical formula, to gauge the seismic capacity of the specimens. Upon comparison with the experimental data, these refined approaches demonstrated superior accuracy in predicting load-carrying capacity compared to traditional analytical models.

1.2.2 Failure mode of splicing structure for shear key

1.2.2.1 Diagonal shear failure

This type of failure often happens in monolithic construction joints, as shown in Figure 1.5. It is mainly determined by the total resistance of vertical reinforcements and hoops crossing inclined cracks. For interior shear keys, the failure happens mainly within the shear key itself. For exterior shear keys, however, the cracks propagate diagonally to the toe of the stem wall. The failure mode of exterior shear keys does not entail sacrificial elements, and considerable damage in the abutment can be expected during a major earthquake. Therefore, this failure mode should be avoided in exterior shear keys.

(a) Interior (Han *et al*., 2018)

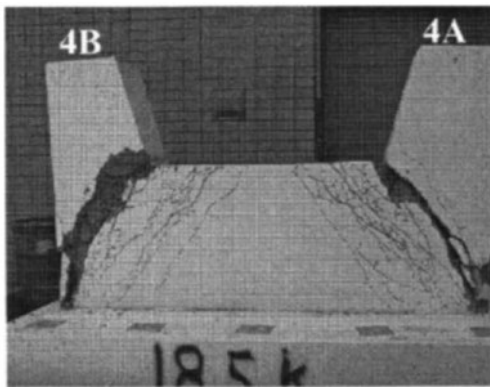

(b) Exterior (Bozorgzadeh *et al*., 2006)

Figure 1.5 Diagonal shear failure mode of shear keys

1.2.2.2 Sliding shear failure mode of shear keys

The sliding shear failure mode is distinguished by the lateral movement of shear keys along their interface with an abutment stem wall. When subjected to a small displacement, numerous diagonal cracks suddenly emerge near the point of loading. Subsequently, additional diagonal cracks manifest on the loading side and progress towards the base of the specimen. At its peak load, the specimen reaches its bearing capacity and then becomes softened due to concrete crushing and spalling. Eventually, the overlay concrete fractures with accompanying interfacial cracks. It is followed by concrete spalling and expansion along the entire length of the specimen, leading to the fracture of some vertical shear key reinforcements, as shown in Figure 1.6(a) and (b), respectively.

(a) Interior (Han *et al*., 2018)

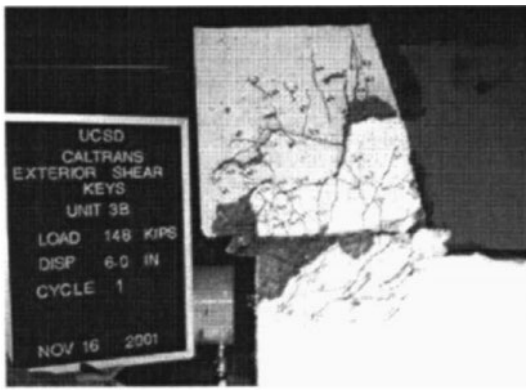

(b) Exterior (Megally *et al*., 2001)

Figure 1.6 Sliding shear failure mode of shear keys

Xiao et al. (2022) performed two series of push-out experiments on shear keys embedded in ultrahigh performance concrete (UHPC). They analyzed damage patterns, load-strain relationships, and other relevant data. The key mechanical parameters of the shear keys were assessed and their mechanical behavior in UHPC were compared with that in normal concrete. Furthermore, the suitability of an established formula for calculating the load capacity of shear keys was examined. During loading, cracks initially formed in the middle of the outer surface of the UHPC blocks. As the load increased, these cracks propagated both upwards and downwards at varying rates of progression, while the widths of the cracks gradually widened. Concurrently, steel fibers were either pulled out or detached from the UHPC. However, no new cracks emerged during this period. Throughout the test, there was a continual increase in relative slip between the steel and the UHPC. In a later stage of loading, this relative slip escalated rapidly, showcasing commendable ductility in the specimen. The ultimate damage observed was the shearing-off of penetrating bars, while the UHPC itself

remained intact aside from the outer vertical cracks, which could effectively serve as a wrapping mechanism for the shear keys.

Figure 1.7 Specimen surface damage patterns (Xiao et al., 2022)

1.2.2.3 Shear friction failure

The shear key acted as a sacrificial component by generating sliding shear friction, thus safeguarding the abutment stem wall from damage. After attaining the maximum strength, horizontal cracks emerged at the base of the sample, accompanied by steep softening due to the failure of the concrete shear keys at the construction joint in this component. As testing progressed in both experimental units, notable sliding of the shear key occurred at the interface between the shear key and the abutment rod wall. There was a slight reduction in bearing capacity as the reinforcement elongated. The vertical reinforcement within the shear key ruptured under increased displacement, resulting in the failure of the shear key. To address this,

the shear keys can be extracted, and new vertical reinforcement can be installed by drilling vertical holes. Subsequently, the holes would be filled with grout and new shear keys would be cast.

(a) Interior (Han *et al*., 2018)

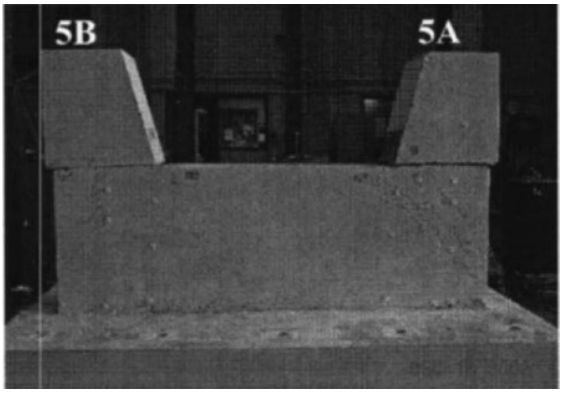

(b) Exterior (Bozorgzadeh *et al*., 2006)

Figure 1.8 Sliding friction failure mode of shear keys

According to Yuan and Chen (2018), a smart shear key is designed to have a pre-made sliding friction failure mode. As a result, the bent cap or abutment will remain undamaged as the shear key absorbs the impact. Following an earthquake, the shear key can be easily replaced. The typical failure mode is presented in Figure 1.9.

Figure 1.9 Failure mode of friction failure mode (Yuan and Chen, 2018)

1.3 ANSYS Model of Shear Keys

ANSYS is a large-scale general-purpose finite element analysis (FEA) software developed by ANSYS, Inc., which was founded in 1970. ANSYS, Inc. focuses on the development of engineering simulation software and technologies. It provides a series of comprehensive software tools ranging from structural simulations through fluid dynamics simulations to electronic designs and simulations. It has been widely adopted for multi-physical field coupled analysis due to its high computational efficiency, flexibility, and convenient operation. ANSYS has been widely used to investigate the response of bridge structures subjected to hydrodynamic forces.

Chapter 2 Computational Model of SMART Shear Keys in a Girder Bridge

The proposed SMART shear keys were tested experimentally and modeled computationally under monotonical loads in Phase I of this multifaceted study (Chen and Yuan, 2020). The effects of SMART shear keys on the seismic responses and nonlinear behavior of a three-span highway girder bridge were modeled and simulated in the OpenSees software platform in Phase II of the study (Zhang et al., 2022). To understand their behaviors under multiple hazards, SMART shear keys were tested under tsunami loads in Phase IV of this study (Zhang et al., 2024). In this report, SMART shear keys' behavior in a concrete girder bridge tested under tsunami loading is modeled and simulated computationally. However, this phase of study started prior to the tsunami testing of the bridge model. As such, the simulation results provide a reference for experimental planning instead of a stand-alone study for the understanding of bridge behavior when SMART shear keys are present.

2.1 ANSYS Simulation Platform

A SMART shear key is designed as a joint to dissipate energy induced by earthquake and/or tsunami loading through friction between Modules I and II, between Modules II and III, and between Module II and dowel bar. The ANSYS software platform is highly efficient in solving nonlinear friction problems. It is used to analyze the contact behavior between various parts of the shear key.

The field of fluid dynamics is governed by a set of mathematical equations known as the Navier-Stokes equations. They are based on the principles of mass conservation, momentum conservation, and energy conservation. With a rapid advancement in computer

technology and software development, commercial software specifically designed for solving these equations is in existence. These software packages are characterized by their user-friendly interfaces, powerful computational capabilities, and high accuracy. Notable examples include CFX, STAR-CD, and FLUENT. The FLUENT module within ANSYS is utilized for simulating solitary waves in numerical simulations.

FLUENT can solve a wide range of problems, including fluid flow, mass and heat transfer, chemical reactions, dynamic deformation of grids, and material processing. It features a non-structured lattice generation sequence that simplifies complex structures into simpler ones for calculation. It includes two-dimensional (2D) trigonal and tetrahedral meshes and three-dimensional (3D) tetrahedral, hexahedral, and hybrid meshes, demonstrating strong adaptability to various boundary conditions. In comparison to traditional numerical methods, the limited volume product method implemented in the software offers excellent stability, wide applicability, and high precision, among other advantages. Notable features include its ability to handle compressible and incompressible flow problems; address steady or unsteady flow scenarios; incorporate a moving grid technology for object movement simulations; offer diverse calculation methods and current modes; support multiphase flow modes such as free surface flow, Eulerian phase flow, and mixed multiphase flow with cavity two-phase flows; accommodate multi-porous dielectric fluid models; and utilize volume source terms grouped by quality processing motion heat and chemistry.

2.2 Computational Model

The superstructure, four SMART shear keys, and the substructure of a 1/5-scale six-girder concrete bridge were modeled (Zhang et al., 2024). To evaluate accuracy and validate the numerical simulations, the bridge model is matched as closely to its represented physical model as possible. The details of the bridge test setup are referred to Zhang et al. (2024).

2.2.1 The superstructure

The superstructure of the experimental bridge model consists of a deck and six girders. In the computational model, it corresponds to bridge deck slabs and girders that are bounded together. The weight of the superstructure in the numerical model is matched to that of the physical model by increasing the density of the material.

The experimental sample of the bridge superstructure was originally designed by Bradner et al. (2011) based on the prototype dimensions of the Escambia Bay I-10 bridge provided by the Florida Department of Transportation. The geometry of the bridge superstructure used in this experiment was 1/5 of the prototype dimensions, as shown in Table 2.1, and the weight of the superstructure was approximately two tons.

Table 2.1 Dimensions of the bridge superstructure

Parameter	**SI (m)**
Width	1.94
Span length	3.45
Deck thickness	0.05
Girder height	0.23
Girder spacing	0.37
Safety barrier height	0.05
Total height at the front edge	0.33

2.2.2 The SMART shear keys

Four SMART shear keys were included in the computational bridge model and distributed outside the two exterior girders to restrain displacements in both directions. Each shear key consists of Module I, Module II, and Module III. Module I and Module II are linked by two horizontally oriented high strength bolts. Similarly, Module II and Module III are linked by two vertically oriented high strength bolts. The vertical contact surfaces of Modules I-II and the horizontal contact surfaces of Modules II-III are not perpendicular to their respective pins in order to control the clamping force at excessive movement. Module III is embedded within the structure of the main beam and firmly fixed.

The smart shear key in the numerical is made from the same materials for each module as that in the experimental model. The pin and each module are linked by a non-separating connection, i.e., frictionless in the tangential direction and non-separable in the normal direction, to simulate the original experimental model in which the pin passes through the modules through a plastic tube.

2.2.3 The substructure

The substructure of the numerical model contains two cap beams. In order to observe the vertical loads at both offshore and onshore locations, vertical load cells were mounted at the lower ends of the cover beams.

2.3 Material Properties

In the computational model, the bridge superstructure and substructure use high strength concrete and steel materials, respectively. In each SMART shear key, Modules I and

III are made of steel (instead of concrete) for easy installation and handling during tests. The potential failure of these two parts may result in the complete failure of the shear key. Module III still uses high strength concrete materials as used in the original design. According to the experimental material tests, the splitting strength and compressive strength of high-strength concrete were 7.4 and 62.3 MPa, respectively, with standard deviations of 0.3 and 2.7 MPa. The yield strength and ultimate tensile strength of the steel bars were 450.0 and 965.8 MPa, respectively, with standard deviations of 3.3 and 32.6 MPa. In these numerical simulations, the compressive and tensile strength of concrete were considered to be 60 MPa and 2 MPa and the yield strength and ultimate tensile strength of the steel dowel bars were 500 and 1000 MPa.

2.4 Assembly and Mesh

The computational model consists of three parts: the superstructure, the shear keys, and the substructure. The superstructure includes the deck slab and the girders, and their contact interface is fixed without slip and deflection. As shown in Figure 2.1, the SMART shear key consists of three modules: I, II, and III in addition to horizontal and vertical reinforcement. The sliding surface of Module II is neither horizontal nor vertical with respect to Module III and Module I, respectively. Its inclination angle is 5º in both directions. The contact interface between reinforcing dowel bars and the modules is free to move tangentially but not detachable in the normal direction to mimic the steel bars covered by a plastic pipe. The contact interface between the cap beam and the shear key is considered a friction surface.

The shear key is fixed to the cap beam by means of pins and bolts. The meshes of the bridge model are shown in Figure 2.2.

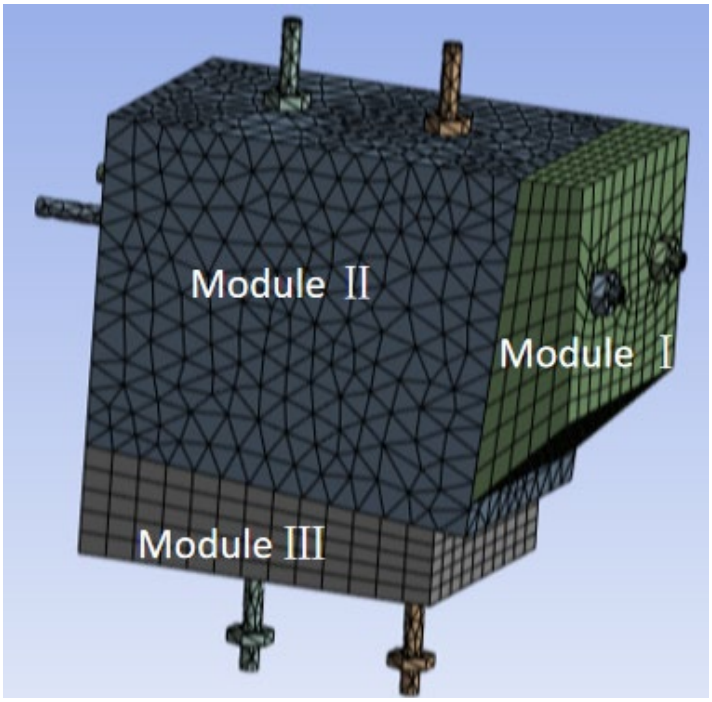

Figure 2.1 Assembly of a SMART shear key

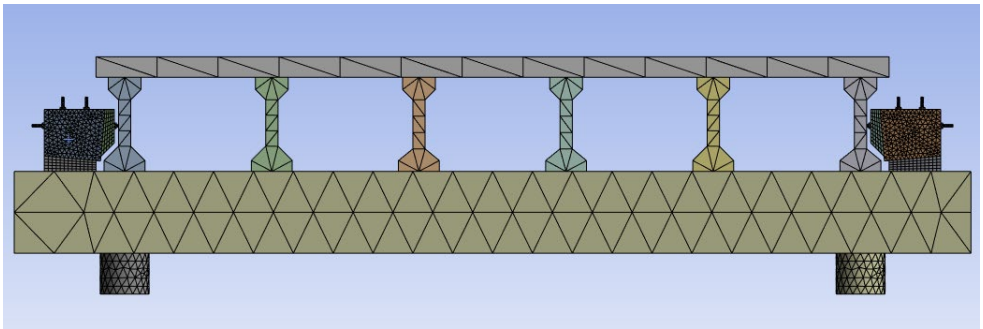

Figure 2.2 Meshing of the bridge model

In the finite element model, the total number of nodes and elements for the 1/5-scale girder bridge and four shear keys are 107,763 and 57,426, respectively. Specifically, the

bridge model has 31,443 nodes and 15,982 elements. The shear key model has 76,320 nodes and 41,444 elements. Tetrahedral elements were used in the bridge deck, six girders, and two cap beams, two cylindrical supports below each cap beam, and Module II of the four shear keys. Tetrahedral elements were selected to mesh complex geometries, such as threaded dowel bars and end nuts, because they can smoothly transition from a coarse mesh to a finer mesh in areas of interest. Hexahedral elements were used in Module I and III of the two shear keys as they are sweepable along one direction in mesh generation.

2.5 Contact Simulation

The computational bridge model involves many contact elements between any two parts: superstructure and shear key, dowel bars and concrete modules in a shear key, two concrete modules in the shear key, and the shear key and substructure. The general goal of contact simulations is to find representative contact areas and calculate representative contact pressure. Under wet conditions, the coefficient of friction between concrete and steel is approximately 0.275. On the surface of a dowel bar against concrete surfaces, friction is dominant in its longitudinal direction and negligible in its transverse direction. There is no separation in the normal direction of the dowel bar and its contacted shear key modules.

For numerical simulations, the transient structure module in ANSYS is used to define the connections between any two parts in the bridge model. To simulate realistic conditions, the contact between the bridge deck and girders is simulated by a binding connection. Reinforcement in the shear key is non-separable with the modules. The connections between

the modules and between Module III and the cap beam are both assigned with friction contacts.

Chapter 3 Simulations of Solitary Wave Impact on the Bridge Model

The computational model of the 1/5-scale six-girder bridge is analyzed under tsunami loading to understand the tsunami effect on the shear key and bridge responses. Both multiphase flow theory and parametric study are presented.

3.1 Three-dimensional Multiphase Flow Model

The bridge model is placed in a large flume to understand the bridge behavior. Considering computational cost effectiveness and isolated wave representation, the flume is set to 40 m long, 1.83 m wide, and 3.2 m high. As illustrated in Figure 3.1, the tsunami wave is generated at the left end of the flume, the bridge model is placed 30 m away from the wave inlet, and the wave outlet is located at the right end after a wave dissipation section. The flume and bridge are proportionally modeled in Geometry—a module in the ANSYS software. The model is imported into ICEM computational fluid dynamics (CFD)—a meshing tool in the ANSYS workbench environment. The flume channel and the bridge model are meshed into hexahedral elements with a global mesh size of 0.2 m and a local refinement size of as small as 0.105 m near the liquid surface and the bridge. The total number of meshes is 419,047.

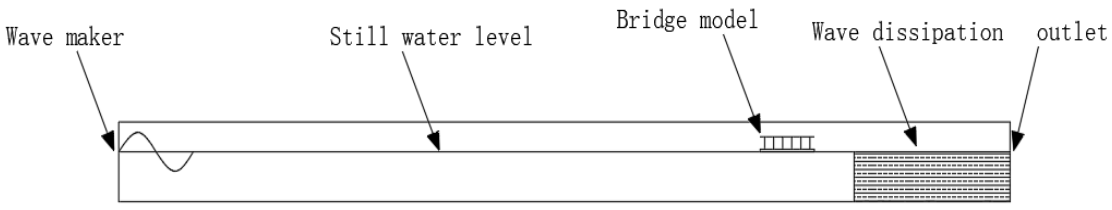

Figure 3.1 Wave flume components and their arrangement

In a viscous wave channel, the wavefront is a water-air interface that changes over time and is impermeable to each other. Since the velocity in the flow field is significantly lower than the speed of sound, both air and water can be treated as incompressible fluids in a 3D multiphase flow model. FLUENT module is chosen for the solution setup to simulate the multiphase flow using the volume of fluid (VOF) method. In the VOF method, a shear stress transport (SST) k-ω turbulence model and a PISO algorithm (i.e., a pressure-velocity coupling scheme) are selected. The wave inlet and outlet are set as velocity and pressure boundary conditions, respectively. In between, the 5^{th}-order solitary wave theory is used for wave generation in the open channel. The free water surface position is set for wave dissipation in the channel. The pressure outlet is set at the top of the flume to ensure air circulation. To ensure calculation accuracy and efficiency, the time step of CFD analysis is set to 0.01 s.

3.2 Natural Frequencies and Mode Shapes

To understand its dynamical properties, the bridge model supported on four cylindrical steel bearings was analyzed using the Model Analysis module in ANSYS. Table 3.1 lists the first five natural frequencies with their corresponding mode shapes shown in Figure 3.2, respectively. The natural frequencies are well spaced.

Table 3.1 The first five natural frequencies of the bridge model

Mode	Frequency (Hz)
1	62.2
2	71.9
3	98.5
4	108.1
5	143.2

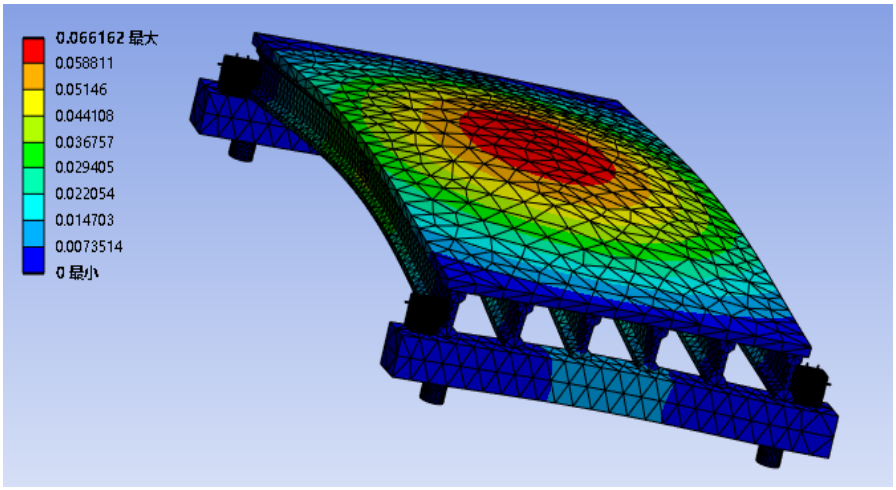

(a) Mode 1

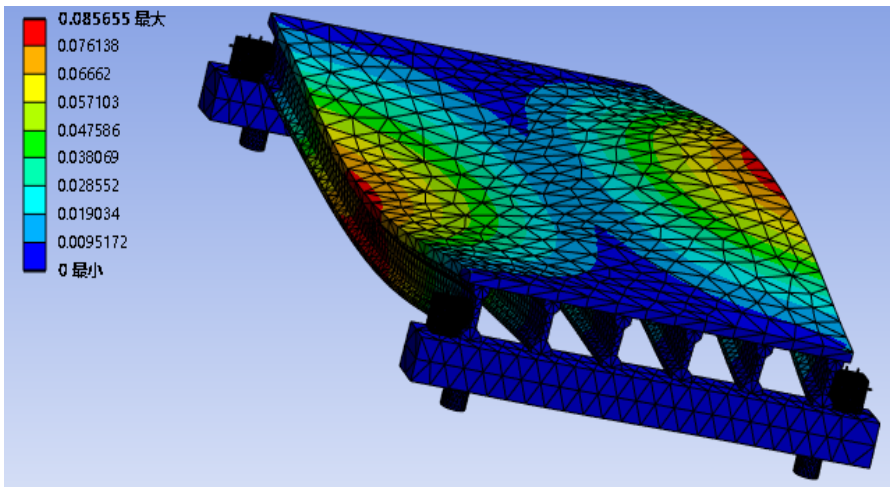

(b) Mode 2

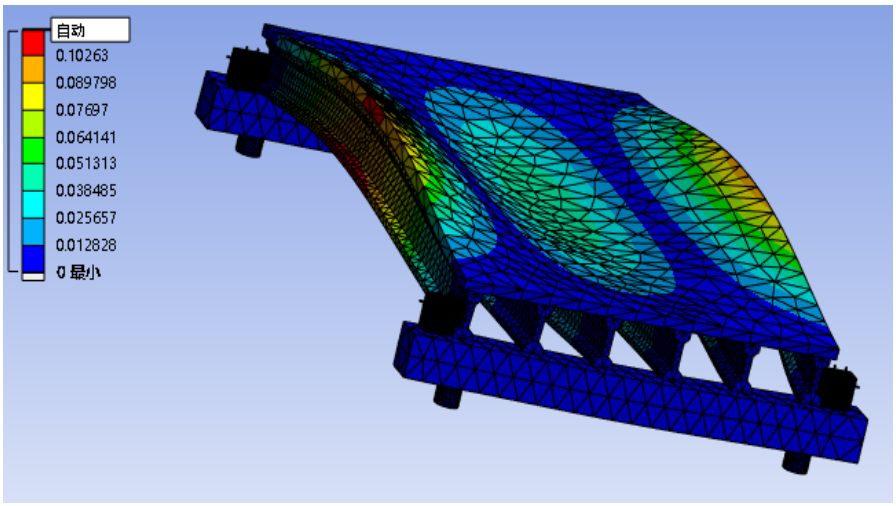

(c) Mode 3

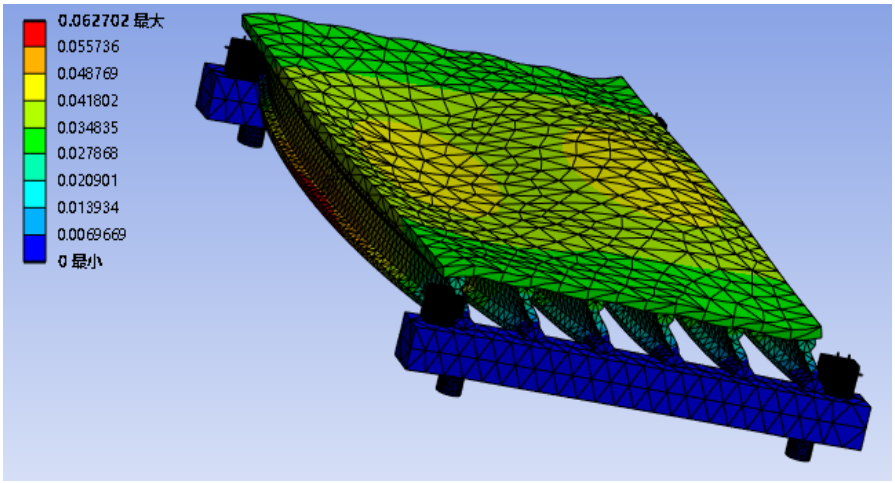

(d) Mode 4

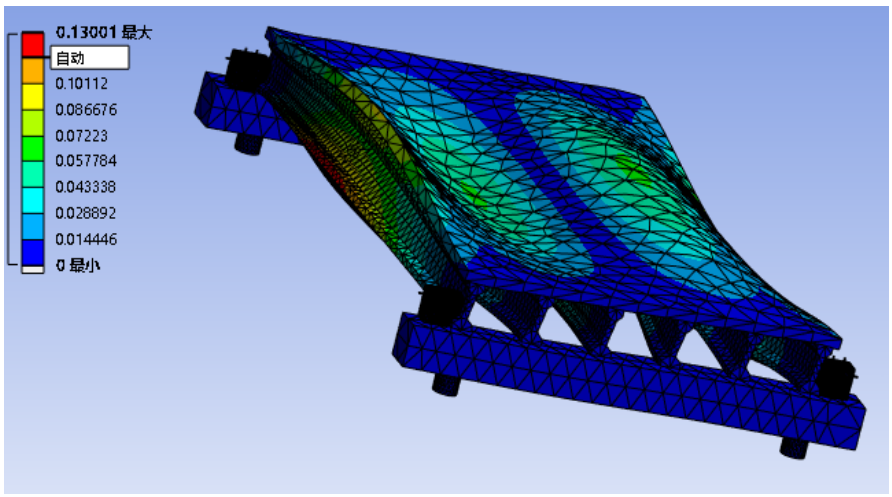

(e) Mode 5

Figure 3.2 First five vibration modes of the bridge model with steel bearings

3.3 Parametric Analysis

Three parameters are investigated to understand their effects on bridge behavior under tsunami loading. These parameters are wave height, friction coefficient of shear keys, and reinforcement strength of dowel bars in the shear keys.

3.3.1 Wave height

Figure 3.3 presents the water-phase cloud diagrams of solitary waves at three wave heights (H = 0.57 m, 0.72 m, and 0.87 m). The impacts of solitary waves on the bridge model with different shear keys are simulated numerically. Figure 3.4 shows the water-phase cloud of the bridge model when impacted by the solitary wave, including three cases when a solitary wave approaches, collides with, and passes the bridge model.

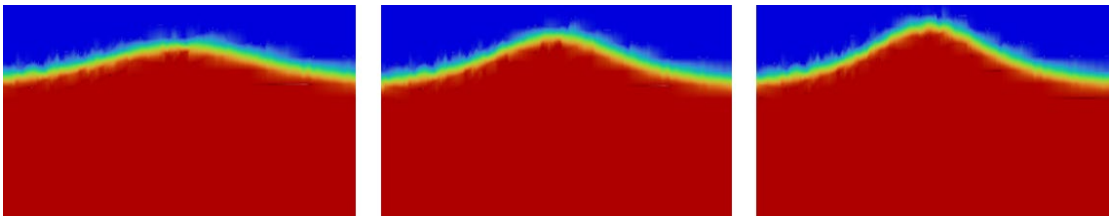

(a) H = 0.57 m (b) H = 0.72 m (c) H = 0.87 m

Figure 3.3 Water-phase cloud diagrams of solitary waves at various heights

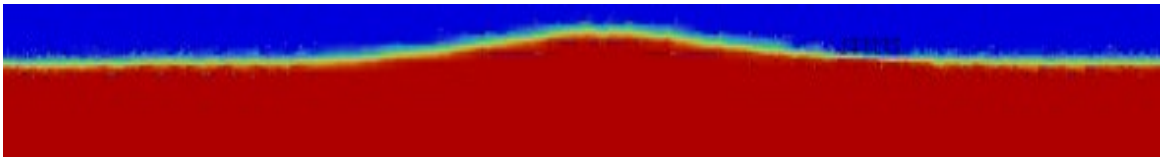

(a) Approaching the bridge

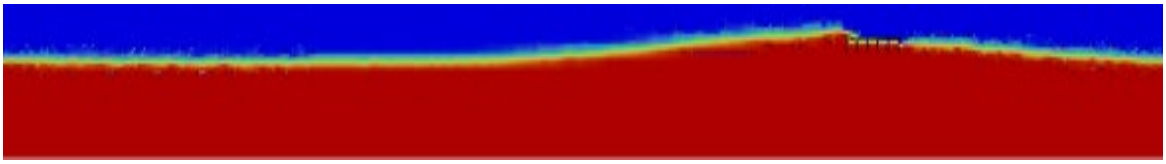

(b) Colliding with the bridge

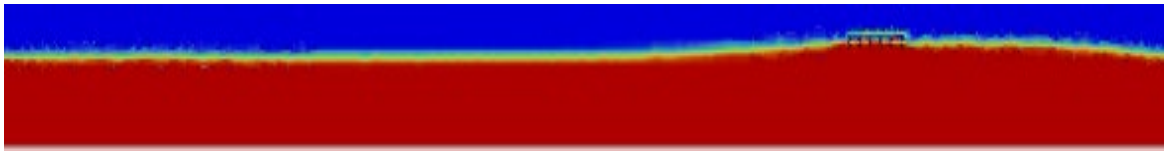

(c) Passing the bridge

Figure 3.4 Water-phase cloud of the bridge model when impacted by as a solitary wave

Based on the solitary wave impacts at different wave heights, the displacement of the bridge deck slab, the horizontal reactions on two steel cap beams, and the vertical reactions on the two beams, the stresses in Module II of the shear keys, and the stresses in the reinforcing bars at both offshore and nearshore locations were analyzed. Figure 3.5 presents the horizontal reaction time histories between 2 s and 7.5 s at three wave heights as a solitary wave approached and passed across the bridge. The entire reaction time history was shifted

upward as the height of a solitary wave increased. Particularly, the reaction amplitude increased significantly with the wave height.

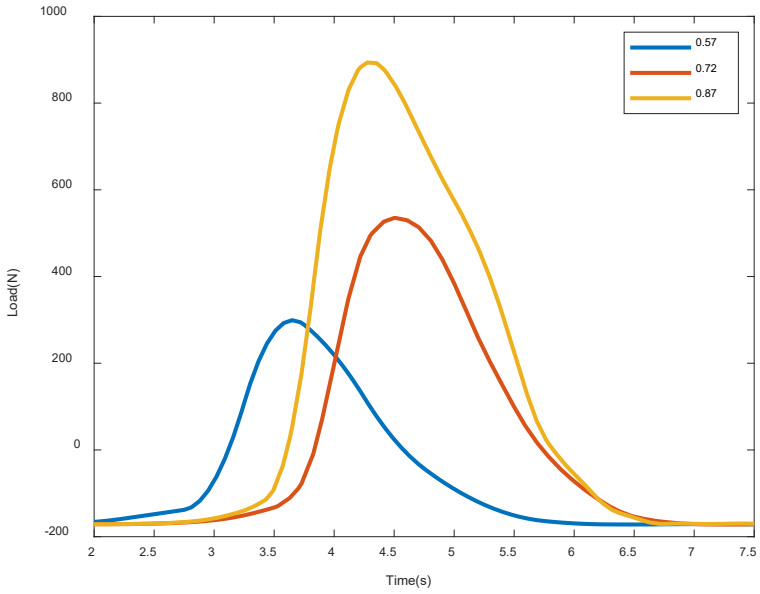

Figure 3.5 Horizontal reaction time histories between 2 s and 7.5 s

Figure 3.6 presents the offshore and onshore vertical reactions between 2 s and 7.5 s. At the beginning of each test, the offshore and onshore reactions were due to gravity effects only. Upon impacting the bridge model, the solitary wave applied an upward force to the bridge, resulting in a reduction of vertical support reactions at both locations. The general trends (shapes) of the two vertical reaction time histories are similar except some local details. The offshore reaction is larger without wave interaction but smaller with wave interaction than the onshore reaction. At either location, offshore or onshore, the reaction amplitude increases with the height of a solitary wave. In comparison with the horizontal reaction time histories, the change in vertical time histories at H = 0.57 m and 0.72 m seems

greater than H = 0.87 m. This comparison likely indicates that the wave-bridge interaction at H = 0.57 m and 0.72 m is stronger than the case at H = 0.87 m.

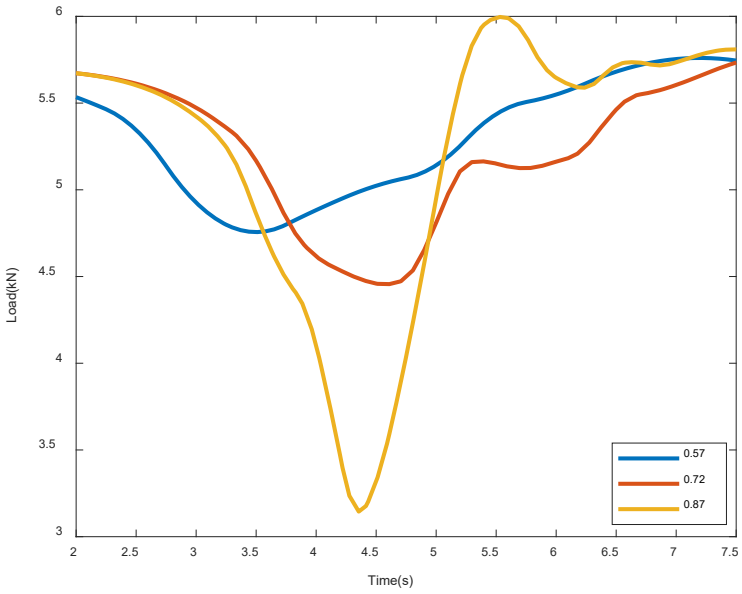

(a) Offshore side

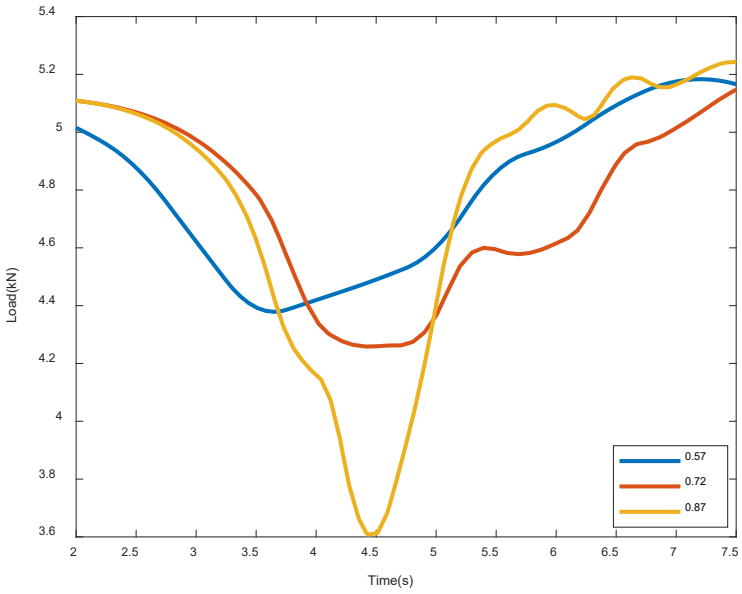

(b) Onshore side

Figure 3.6 Vertical reaction time histories between 2 s and 7.5 s: (a) offshore and (b) onshore

The impact of the solitary wave on the bridge model causes slippage in the shear keys and displacement in the bridge model. The bridge deck displacement at each wave height and the shear slip of Module II are presented in Figures 3.7 and 3.8, respectively. It can be observed that the displacement variation increases with the wave height. At H = 0.57 m and 0.72 m, the change in deck displacement is significantly smaller than that at H = 0.87 m. Once again, this comparison indicates stronger wave-bridge interaction at the two lower wave heights.

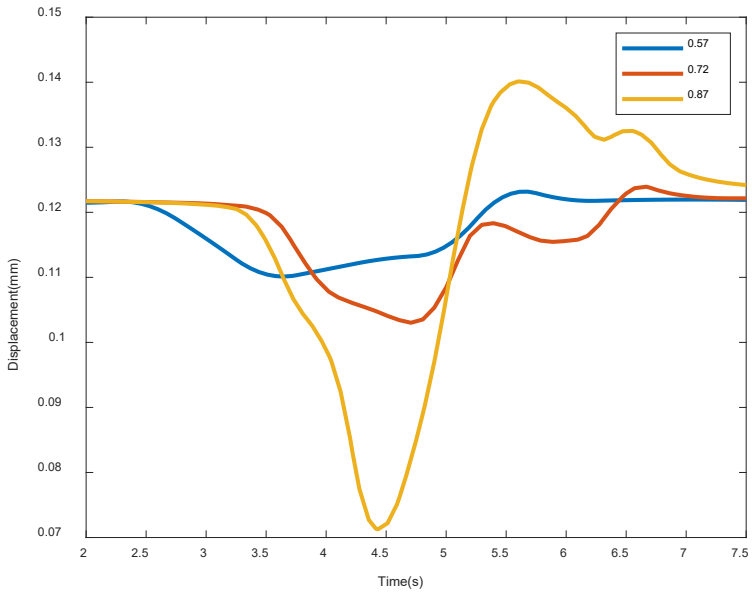

Figure 3.7 Displacement of the bridge deck

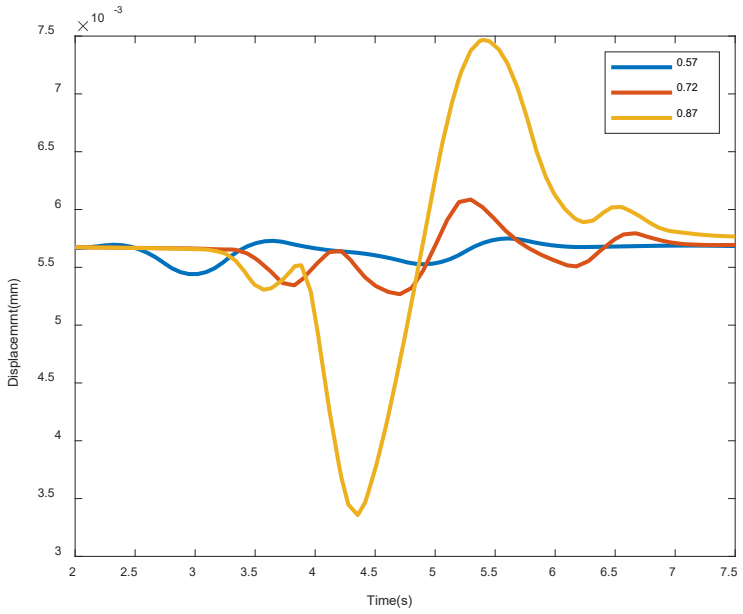

(a)

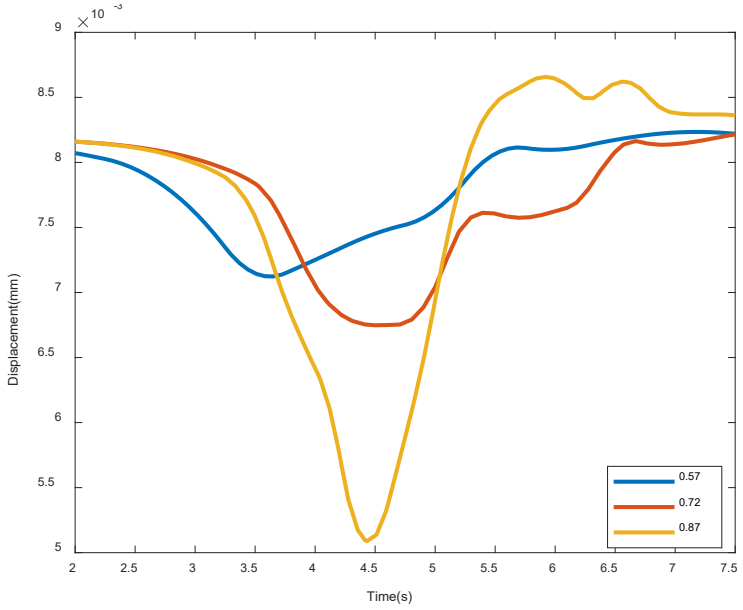

(b)

Figure 3.8 Displacement (slip) of shear key Module II: (a) offshore and (b) onshore

When subjected to a solitary wave, various modules of the shear keys experience relative motion and thus load the dowel bar. The time histories in maximum principal stress of the dowel bar reinforcement at the offshore and onshore locations are presented in Figure

3.9. It can be seen that the minimum principal stress of the time history decreases with the wave height, which is particularly clear in the onshore shear key. The principal stress in the offshore shear key varies more significantly than that in the onshore shear key. This is because the solitary wave at the offshore location is likely broken more frequently due to stronger wave-bridge interaction.

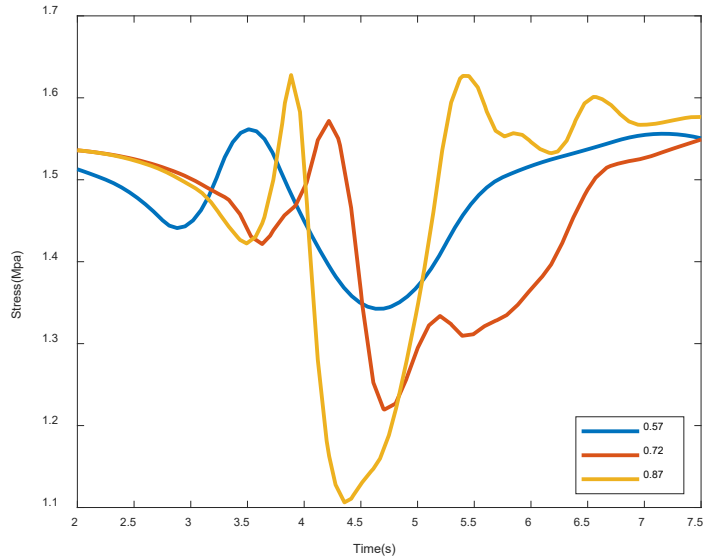

(a)

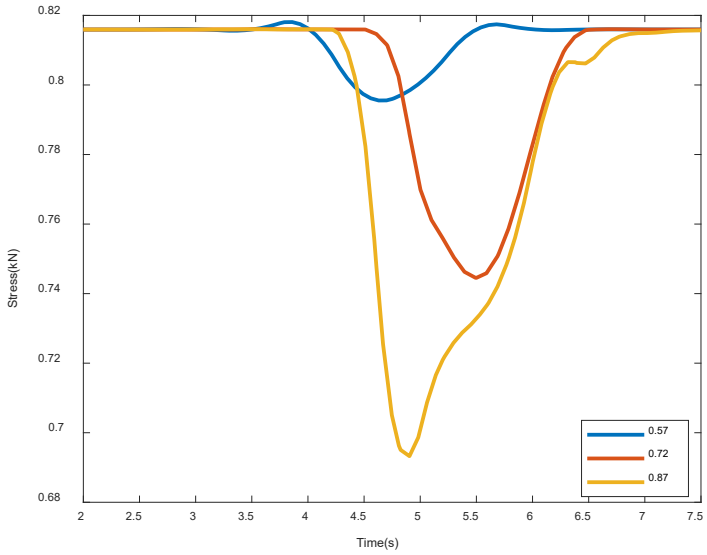

(b)

Figure 3.9 Dowel bar principal stress in shear keys: (a) offshore and (b) onshore

3.3.2 Friction coefficient

To be more controllable on the bridge model and shear keys during experimental tests, Modules I and III were made of steel plates instead of fiber-reinforced concrete as originally designed. Module III was fixed, and Module II placed on top of Module III was laterally pulled to slide at a nearly constant speed. Based on the friction force measured by an electric scale, the coefficient of friction between the fiber-reinforced concrete and the steel was $\mu_f = 0.367$, which was slightly lower than 0.4 between two dry fiber-reinforced concrete components. To mimic the wet working environment of the shear keys under tsunami loading, water was splashed on the interface of Modules II and III. Under the wet condition, μ_f was reduced to 0.275.

To investigate its effect on the tsunami responses of the bridge, the friction coefficients at the interface of shear key modules is taken to be 0.275, 0.325, and 0.375. These values correspond to the experimental measurement and the deformation of shear key Module II (and then normal force on the friction surface) as observed at H = 0.72 m. Figure 3.10 presents the displacement time histories of Module II of the shear key at all levels of friction coefficient. It can be observed from Figure 3.10 that the onshore displacement is substantially greater than the offshore displacement. This is because the hydrodynamic force pointing from the offshore to onshore side is applied to the shear key on the onshore side only. Furthermore, the Module II displacement on the offshore side decreases significantly with the increase of the friction coefficient between two modules of the shear key. On the onshore side, the Module II displacement decreases slightly with the increase of friction

coefficient. On both the offshore and onshore sides, the effect of friction coefficient on the shear key displacement becomes negligible after the friction coefficient exceeds 0.3.

It can also be observed from Figure 3.10(b) that the Module II maintains a nearly constant displacement near 5.5 s. This is likely because the Module II experiences sliding to sticking to sliding again against its connecting dowel bars as the solitary wave passes through the bridge model. In addition, both shear keys on the offshore and onshore sides seem re-set into the original position after the passage of the solitary wave, leaving behind little permanent displacement and thus making the bridge with SMART shear keys are more resilient than traditional shear keys.

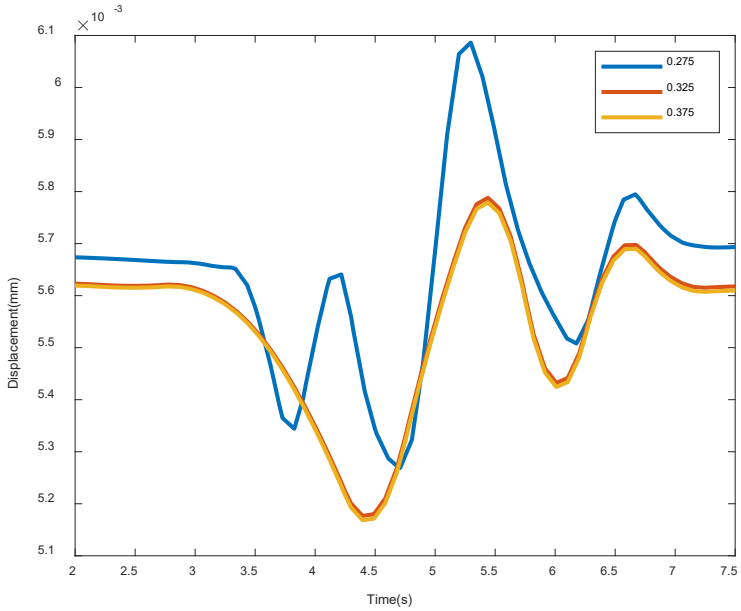

(a) Offshore side

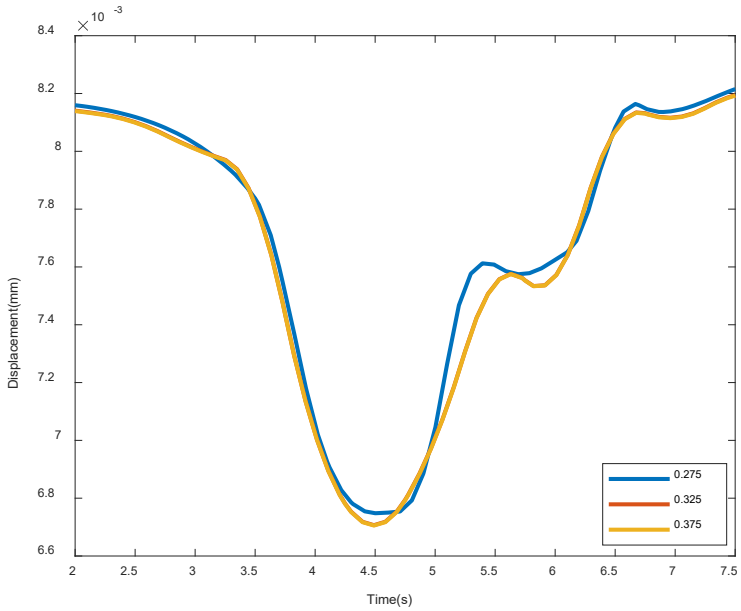

(b) Onshore side

Figure 3.10 Displacement time histories of Module II of the shear key: (a) offshore and (b) onshore

Chapter 4 Concluding Remarks

In this report, SMART shear keys are briefly reviewed as fuse elements in girder bridges. The novelty in SMART shear keys is thy provide a tradeoff between the girder movement and the load transferred from the bridge substructure to substructure. The positive device that is intentionally designed to manage displacement and force through the mechanism of controllable friction is first of its kind in bridge applications under tsunami loading. Based on the numerical results, the following conclusions can be drawn:

1. Under the impact of solitary waves, the maximum horizontal reaction and the minimum vertical reaction of the bridge model increase with the wave height. The wave-bridge interaction at a wave height of H = 0.57 m and 0.72 m appear stronger than that at H = 0.87 m, which is related to characteristics specific to the bridge model. This observation is supported by the simulated deck displacement responses.
2. In SMART shear keys, the slip responses between the main module (II) and the base module (III) on the onshore side indicate a sliding-sticking-sliding phase transformation. The SMART shear keys on both offshore and onshore sides experience self-resetting after the passage of a solitary wave due to prestressed dowel bars. Dowel bar stress and the shear slips all indicate that the shear key on the offshore side went through more complex behavior than the shear key on the onshore side.
3. The displacement of shear keys due to a solitary wave is affected by the choice of friction coefficient at the interface between two modules of a shear key unless the

friction coefficient exceeds 0.3. The slip response time history also confirms that the shear key on the offshore side varies more dramatically than that on the onshore side.

Although this report provides some insights on how the bridge model with four SMART shear keys responds to solitary waves, further studies are required to compare the computational results with experimental data (Zhang et al., 2024). The bridge model also needs to be refined to better represent the physical model tested in Zhang et al. (2024). The scale effect from the bridge model to its prototype (Martinelli et al., 2010; Takahashi et al., 1985) needs to be investigated.

For engineering applications, two critical factors must be investigated. First, current findings are limited to the effect of unbroken solitary waves only. More realistic tsunami-like bores considering the difference in wavelength (Madsen et al., 2008; Madsen and Schaffer, 2010; Chan and Liu, 2012) and applied force (Leschka and Oumeraci, 2014; Istrati and Buckle, 2019) must be studied. Second, a comprehensive design method and procedure must be formulated for a controllable tradeoff of deck displacement and substructure force under multiple hazards, such as earthquake and tsunami loads.

References

Bozorgzadeh, A., Megally, S., Restrepo, I.J., et al. 2006. Capacity Evaluation of Exterior Sacrificial Shear Keys of Bridge Abutments. Journal of Bridge Engineering 11(5):555-565.

Bradner, C., Schumacher, T., Cox, D., and Higgins, C. 2011. Experimental Setup for a Large-scale Bridge Superstructure Model Subjected to Waves. Journal of Waterway, Port, Coastal, Ocean Engineering 137 (1): 3 – 11. https://doi.org/10.1061/(ASCE)WW.1943-5460.0000059.

CALTRANS. 2019. Seismic Design Criteria, Version 2.0, California Department of Transportation, Sacramento, CA

Chan, I. C., and Liu, L.F. 2012. On the Runup of Long Waves on a Plane Beach. Journal of Geophysical Research: Oceans 117 (C8): C08006. https://doi.org/10.1029/2012JC007994.

Chen, G. and Yuan, X.Z. 2020. SMART Shear Keys for Multi-Hazards Mitigation of Diaphragm-Free Girder Bridges - Phase I: Design and Characterization. Final Report to Mid-America Transportation Center, University of Nebraska-Lincoln, December 31, 2020.

Han, Q., Zhou, Y., Ou, Y., & Du, X. 2017. Seismic Behavior of Reinforced Concrete Sacrificial Exterior Shear Keys of Highway Bridges. Engineering Structures 139: 59–70. https://doi.org/https://doi.org/10.1016/j.engstruct.2017.02.034

Han, Q., Hu, M.H., Zhou, Y.L., & Du, X.L. 2018. Seismic Performance of Interior Shear Keys of Highway Bridges. ACI Structural Journal 115(4): 1011–1021. https://www.concrete.org/publications/internationalconcreteabstractsportal/m/details/id/51701916

Han, Q., Hu, M.H., Wen, J.N., & Du, X.L. 2020. Seismic Capacity Evaluation of Interior Shear Keys for Highway Bridges. Journal of Earthquake Engineering 24(6): 972–987. https://www.tandfonline.com/doi/abs/10.1080/13632469.2018.1453414

Hayatdavoodi, M., Seiffert, B., and Ertekin, R.C. 2014. Experiments and Computations of Solitary-wave Forces on a Coastal-bridge Deck. Part II: Deck with Girders. Coastal Engineering 88: 210-228. https//doi.org/10.1016/j.coastaleng.2014.02.007

Istrati, D., and Buckle, I.G. 2019. Role of Trapped Air on the Tsunami-induced Transient Loads and Response of Coastal Bridges. Geosciences 9 (4): 191.

https://doi.org/10.3390/geosciences9040191.

Istrati, D., Buckle, I.G., Lomonaco, P., and Yim, S. 2018. Deciphering the Tsunami Wave Impact and Associated Connection Forces in Open-girder Coastal Bridges. Journal of Marine Science and Engineering 6 (4): 148. https://doi.org/10.3390/jmse6040148.

Kottari, A., Shing, P.B., & Bromenschenkel, R. 2020. Shear Behavior of Exterior Non-Isolated Shear Keys in Bridge Abutments. ACI Structural Journal 117(2): 225–237. https://www.concrete.org/publications/internationalconcreteabstractsportal.aspx?m=details&id=51721317

Kottari, A., Mavros, M., Murcia-Delso, J., and Shing, P.B. 2017. Interface Model for Keys-slip and Dowel-action Behavior. ACI Structural Journal 114 (4):1043 – 1053. https://doi.org/10.14359/51689870.

Leschka, S., and Hocine, O. 2014. Solitary Waves and Bores Passing Three Cylinders-effect of Distance and Arrangement. Proceedings of the 34th International Conference on Coastal Engineering. New York: Curran Associates.

Madsen, A., Fuhrman, D.R., and Schäffer, H.A. 2008. On the Solitary Wave Paradigm for Tsunamis. Journal of Geophysical Research.: Oceans 113: C12012. https://doi.org/10.1029/2008JC004932.

Madsen, A., and Schäffer, H.A. 2010. Analytical Solutions for Tsunami Run-up on a Plane Beach: Single Waves, N-waves and Transient Waves. Journal of Fluid Mechanics 645: 27 – 57, February, 2010. https://doi.org/10.1017/S0022112009992485.

Martinelli, L., Lamberti, A., Gaeta, M.G., Tirindelli, M., Alderson, J., and Schimmels, S. 2011. Wave Loads on Exposed Jetties: Description of Large Scale Experiments and Preliminary Results. Coastal Engineering Proceedings 32: 18, January 29, 2011. https://doi.org/10.9753/icce.v32.structures.18.

Megally, S., Silva, P., & Seible, F. 2001. Seismic Response of Sacrificial Shear Keys in Bridge Abutments. UCSD/SSRP-2001/23, University of California, San Diego. Department of Structural Engineering.

Reid, J.A. and Mooney, W.D. 2023. Tsunami Occurrence 1900–2020: A Global Review, with Examples from Indonesia. Pure and Applied Geophysics 180: 1549–1571.

Silva, P. F., Megally, S., & Seible, F. 2009. Seismic Performance of Sacrificial Exterior Shear Keys in Bridge Abutments. Earthquake Spectra 25(3): 643–664. https://journals.sagepub.com/doi/abs/10.1193/1.3155405

Takahashi, S., Tanimoto, K., and Miyanaga, S. 1985. Uplift Wave Forces due to Compression of Enclosed Air Layer and their Similitude Law. Coastal Engineering in Japan 28 (1): 191 – 206. https://doi.org/10.1080/05785634.1985.11924415.

Xiao, L., Liao, X., Wei, X., and Chen, F. 2022. Experimental Study on Mechanical Properties of PBL Shear Connectors in UHPC. Journal of the China Railway Society 44(12): 157-164. (In Chinese)

Yuan, X., and Chen, G. 2018. An Adaptive SMART Shear Key and its Mechanical Properties for Earthquake/Tsunami Mitigation. Proceedings of the 7th World Conference on Structural Control and Monitoring, Qingdao, China.

Yuan, X., Zhu, Y., Chen, G., Zhang, H., Chen, Z., and Fan, L. 2019. SMART Shear Keys to Prevent Bridge Girders from Falling off during Earthquakes and Tsunami — Preliminary Numerical Simulations. Proceedings of the 3rd International Bridge Seismic Workshop, Z ü rich, Switzerland, International Association of Bridge Earthquake Engineering.

Zhang, H.B., Yuan, X.Z., Mondal, T.G., and Chen, G. 2022. SMART Shear Keys for Multi-Hazards Mitigation of Diaphragm-Free Girder Bridges - Phase II: Numerical Simulation on Seismic Performance. Final Report to Mid-America Transportation Center, University of Nebraska-Lincoln, July 6, 2022.

Zhang, H.B., Tie, R.T., Chen, G., and Yuan, X.Z. 2024. SMART Shear Keys for Tsunami/Storm Surge-Hazards Mitigation of Concrete Girder Bridges. Final Report to Mid-America Transportation Center, University of Nebraska-Lincoln, June 14, 2024.